Journal of Computational Electronics (2021) 20:1006–1011
https://doi.org/10.1007/s10825-021-01657-z

Improvement of RF MEMS devices by spring constant scaling laws

Deepak Bansal[1] · **Prem Kumar**[1] · **Amit Kumar**[1]

Received: 23 July 2020 / Accepted: 9 January 2021 / Published online: 2 February 2021

Abstract
The technology for radio frequency micro-electro-mechanical system (RF MEMS) is well established. In the next phase of miniaturization, RF MEMS transforming into RF nano-electro-mechanical system (NEMS) requires scaling laws. For MEMS devices, vertical scaling laws are available in the literature. However, existing scaling laws are isotropic and not valid for the majority of the MEMS devices. Like VLSI technology, the scaling in the MEMS is asymmetric and needs optimization in each direction. In the MEMS, depending upon the working principle, the scaling laws vary from device to device. In the present work, spring constant scaling laws for the electrostatic RF MEMS devices are derived given the device performance. The scaling laws are derived in such a way that existing limitations of the MEMS technology like low switching speed, high pull-in voltage, stiction, etc., are minimized and the response of the switch is improved.

Keywords Scaling law · Miniaturization · MEMS · Spring constant

1 Introduction

Since the last decades, the miniaturization of gadgets is in trend and big systems are converting into small chips and portable devices [1–4]. Going down from bigger to smaller dimensions with the same governing laws is called scaling. The scaling in a VLSI technology is well known, and technology for lower than 9 nm has been achieved. Like Moore's law in VLSI, dimensions of the MEMS devices are also reducing year by year and moving toward NEMS. Miniaturization without proper laws leads to unwanted results and degrades device performance. Vertical isotropic scaling laws [3, 4] are proposed for the MEMS devices. However, MEMS devices are anisotropic means all the parameters are not scaled by the same factor. The device parameters like pull-in voltage, mechanical and electrical frequency, power consumption, speed, and lifetime are correlated with each other. These parameters are dependent upon basic parameters like length, width, and thickness [5, 6]. Any change in basic parameters will alter the functioning of the device. In MEMS, depending upon the working principle, scaling laws vary from device to device [7–10]. In the present paper, the generalized scaling laws are explored for RF MEMS devices for improvement in device performance. RF response of the MEMS devices is better than solid-state devices. However, electro-mechanical parameters, e.g., low switching speed, high operating voltage, stiction probabilities, are limiting factors for the MEMS devices. In addition to scaling, these limiting factors are also addressed.

2 RF MEMS Scaling

RF MEMS devices have advantages of low power consumption, high isolation, low insertion, and high linearity over the solid-state devices. RF MEMS switch is a basic building block for the majority of the RF devices, e.g., varactor, t-matrix, and phase shifter [11–14]. The scaling laws applicable to the RF MEMS switch are also applicable to other RF MEMS devices. In the present paper, generalized scaling for the RF MEMS switch is performed which is applicable for most of the RF MEMS components. The scaling laws are formed in such a way that existing limitations of the MEMS devices like low speed, high actuation voltage, low mechanical response, power handling, and self-actuation are minimized as described below:

✉ Deepak Bansal
deepak@ceeri.res.in

[1] CSIR-Central Electronics Engineering Research Institute, Pilani 333031, Rajasthan, India

2.1 Pull-in voltage

One of the major limitations of the RF MEMS devices is high pull-in voltage which needs to be scaled down. The pull-in voltage (V_p) of the RF MEMS switch is given by

$$V_p = \sqrt{\frac{8kg^3}{27\varepsilon_o w L_{el}}} \tag{1}$$

where ε_o is the permittivity of free space. g, w, and L_{el} are a gap, width of structure/pull-in electrode, and length of electrode, respectively, as shown in Fig. 1. And k is a spring constant which is a function of structural geometry and force as listed in Table 1.

A generalized formula for spring constant is given by

$$k = C_1 Ew\left(\frac{t}{L}\right)^3 \tag{2}$$

where C_1 is geometry/load dependent constant and E is Young's modulus of the material. w and t are the width and thickness of the bridge/cantilever. The actuation electrode width (w) is taken equal to the cantilever width to reduce actuation voltage.

Combining equations (1) and (2)

$$V_p = \sqrt{C_1 \frac{8g^3 E}{27\varepsilon_o L_{el}}\left(\frac{t}{L}\right)^3} \tag{3}$$

With scaling, we can reduce its pull-in voltage.

From equations (2) and (3), scaling of 't and L' by 'β (< 1)' would not change k and V_p. The scaling of 'w' would reduce k or stiffness which degrades its reliability. Hence, width (w) of the structure is kept constant and other parameters (t, L, and L_{el}) are scaled by β.

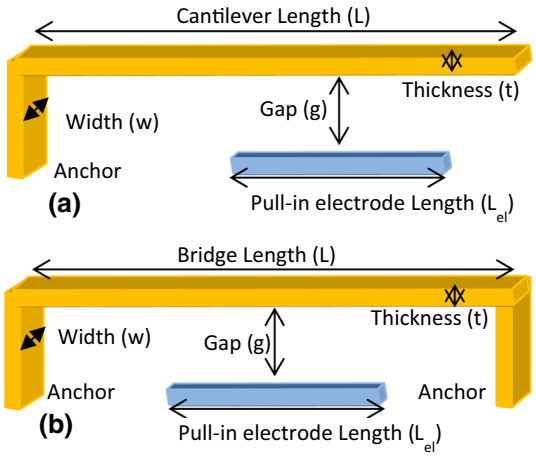

Fig. 1 3D schematic of (**a**) cantilever- and (**b**) bridge-based MEMS devices

Table 1 Spring constant for commonly used MEMS structures

SN	Boundary condition	Load type	Spring constant
1	Clamped-free (cantilever)	Point end load	$k = \frac{1}{4}Ew\left(\frac{t}{L}\right)^3$
2	Clamped-free (cantilever)	Uniform load	$k = \frac{2}{3}Ew\left(\frac{t}{L}\right)^3$
3	Clamped–clamped (bridge)	Point load at the middle	$k = 16Ew\left(\frac{t}{L}\right)^3$
4	Clamped–clamped (bridge)	Uniform load	$k = 32Ew\left(\frac{t}{L}\right)^3$

Scaling of 'g' is different from 't' and 'L' as 'g' affects the RF isolation and involves fabrication complexities [15]. Hence, the scaling of 'g' is done with another factor α (< β). All the scaled parameters are listed in Table 2. With scaling, scaled spring constant (k_s) and scaled actuation voltage ($V_{p,s}$) become

$$k_s = k \tag{4}$$

$$V_{p,s} = \sqrt{\frac{\alpha^3}{\beta}} V_p \tag{5}$$

Here, scaling is different in all three directions and optimized for RF MEMS switch applications.

Simulations are performed on CoventorWare software to verify the scaling laws.

The value of β and α is chosen ½ and 1/1.5, respectively, for the sake of simplicity. The original cantilever of parameters $400 \times 50 \times 3$ μm^3 is taken and scaling according to Table 2. 3D views of the original and scaled cantilevers are shown in Fig. 2. Here, scaling-1 means scaled by factor β and α, scaling-2 means scaled by factor β^2 and α^2, and so on. The scaling is called spring constant scaling as spring stiffness is not compromised and kept fixed as shown in Fig. 3.

Table 2 The scaling laws ($\beta < \alpha < 1$) for the physical parameters of the switch

S.N	Physical parameter	Scaling factor
1	Switch length (L)	β
2	Switch width (w)	1
3	Switch thickness (t)	β
4	The gap between electrode and cantilever (g)	α
5	Pull-in electrode length (L_{el})	β
6	Pull-in electrode width (w)	1
7	Dielectric thickness (t_d)	1

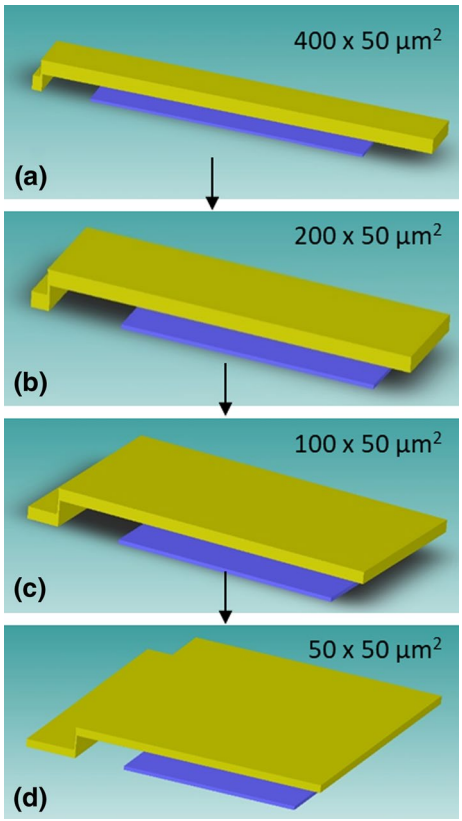

Fig. 2 3D view of (**a**) original, (**b**) scaled-1, (**c**) scaled-2 and **d** scaled-3 cantilevers

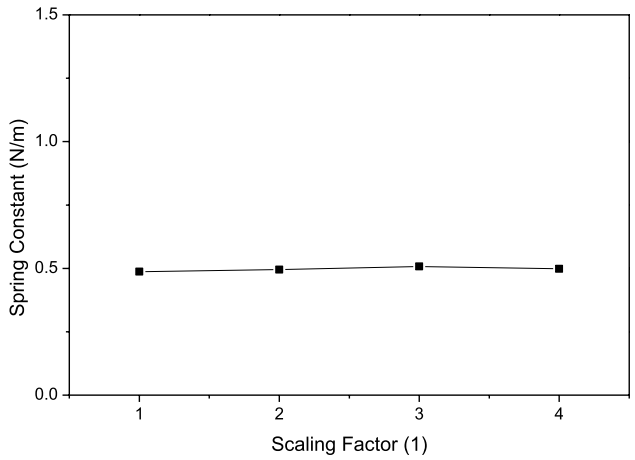

Fig. 3 Negligible change in the spring constant with the scaling

The pull-in voltage of the switch decreases from 12.75 V to 5.25 V with scaling as shown in Fig. 4 which is a good achievement for the MEMS devices.

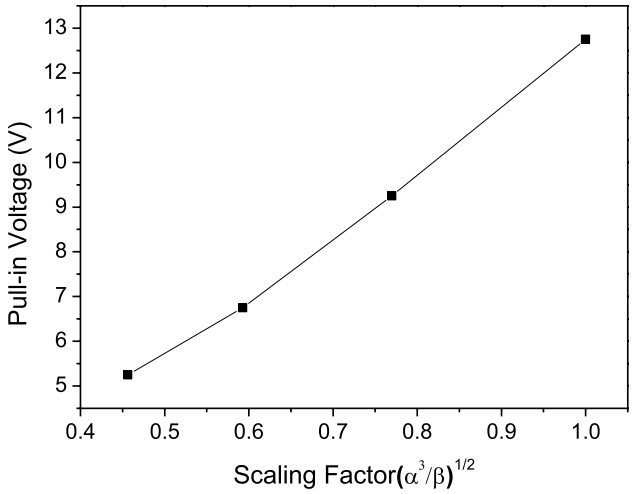

Fig. 4 Pull-in voltage scaling for the switch

2.2 Restoring force

The MEMS cantilever/bridge is moved down with the help of electrostatic force and moves upward with restoring force of the structure. If the restoring force is less, the cantilever will stick in its down position. Hence, restoring force should not degrade with scaling. The restoring force (F_{res}) for the mechanical structure is given by

$$F_{res} = -kx \tag{6}$$

where 'x' is the displacement of the MEMS structure. The maximum restoring force in downstate position is

$$F_{res,\max} = -kg \tag{7}$$

where 'g' is the gap between the electrode and cantilever/bridge which is equal to the maximum possible displacement of the structure. With scaling, from equation (4) and Table 2, scaled restoring force ($F_{res,s}$) would decrease by α.

$$F_{res,s} = \alpha F_{res} \tag{8}$$

However, stiction forces that are proportional to the contact area also decrease by a factor of β which is less than α. In other words, there is an overall improvement in the stiction probabilities of the switch.

2.3 Mechanical frequency

The mechanical resonance frequency (f) of the switch should be large for the quick response and is given by

$$f = \frac{1}{2\pi}\sqrt{\frac{k}{m}} = \frac{1}{2\pi}\sqrt{\frac{C_1 Ew}{\rho Lwt}\left(\frac{t}{L}\right)^3} = \frac{1}{2\pi}\frac{t}{L^2}\sqrt{C_1\frac{E}{\rho}} \tag{9}$$

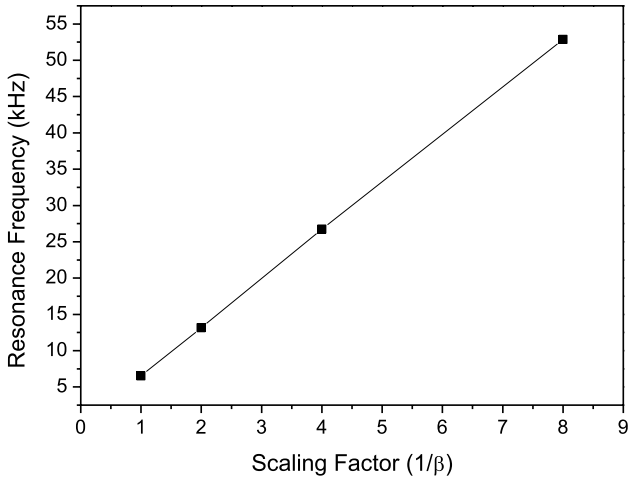

Fig. 5 Improvement in the mechanical resonance frequency with the scaling

and scaled mechanical frequency (f_s) is

$$f_s = f/\beta \tag{10}$$

The mechanical resonance frequency of the structure increases by a factor of 1/β which makes the device fast. The simulated result for the resonance frequency is shown in Fig. 5. The resonance frequency of the switch improves from 6.5 kHz to 52.9 kHz.

2.4 Switching speed

The switching speed of the MEMS devices is slow as compared to solid-state devices. The scaling is done in such a way that it would help in improving the speed.

The switching speed for the switch is a function of damping. The switching time (t_{od}) for overdamped system $Q < 0.5$, is given [12] by

$$t_{od} = \frac{2bg^3}{3\varepsilon_o A V_s^2} = \frac{9V_p^2}{8\pi f Q V_s^2} \tag{11}$$

where b and Q damping constant and quality factor. V_p and V_s are pull-in and supplied voltage.

After scaling, the scaled switching time ($t_{od,s}$) for the overdamped system is given by

$$t_{od,s} = \beta t_{od} \tag{12}$$

On the other hand, the switching time (t_{ud}) for an underdamped system ($Q > 2$) is given by,

$$t_{ud} = 3.67\frac{V_p}{V_s \omega_o} \tag{13}$$

After scaling, the scaled switching time ($t_{ud,s}$) of the switch improves by β.

$$t_{ud,s} = \beta t_{ud} \tag{14}$$

The simulated switching speed results are shown in Fig. 6. The switching speed improves from 52 µsec to 6.6 µsec with scaling.

2.5 Power consumption

The power consumption (P) of the electronics component is given by

$$P = I^2 R \tag{15}$$

where I and R are current and resistance.

In the case of an RF MEMS switch, the actuation voltage is applied through the dielectric material and there is no direct flow of current. Hence, the resistive power consumption is zero. However, the dielectric material between the MEMS structure and the actuation electrode leads to the formation of a capacitor. The energy (E_{energy}) lost through the capacitor is given by

$$E_{energy} = \frac{CV_p^2}{2} = \frac{1}{2}\frac{\varepsilon_o w L_{el}}{g} V_p^2 \tag{16}$$

where C is the capacitance between cantilever/bridge and actuation electrode.

After scaling, the scaled energy ($E_{energy,s}$) consumption is given by

$$E_{energy,s} = \alpha^2 E_{energy} \tag{17}$$

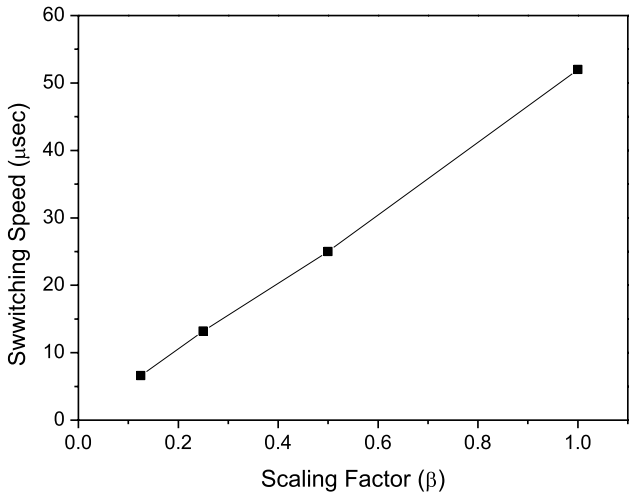

Fig. 6 Improvement in the switching speed with the scaling

With scaling, energy consumption is also reduced by a factor of α^2.

2.6 Stiction forces

In the MEMS devices, the cantilever/bridge moves down with the actuation voltage and contacts the bottom layer. Due to some forces called stiction forces like capillary, dielectric stiction, and van der Waals, etc., the structure may stick in its down position. These stiction forces are directly proportional to a contact area (wL) [15, 16]. With scaling, length decreases by β, and width remains constant as listed in Table 2. Hence, both the contact area and the stiction forces would decrease by β, and the reliability of the device gets improved. In the proposed design, the contact area decreases from $20\times50\ \mu m^2$ to $2.5\times50\ \mu m^2$ which reduces the stiction probabilities.

With scaling, from equation (17), capacitive coupling forces are reduced by α^2. The dielectric stiction forces are directly proportional to capacitive coupling [17–19]. Hence, the dielectric stiction force is further decreased by α^2.

2.7 Power handling limited by Self-actuation

The pull-in voltage required for actuation of the switch is given by [12]

$$V_p = \sqrt{\frac{8kg^3}{27A\varepsilon_o}} \tag{18}$$

where A is an area of overlap between the cantilever/bridge and electrode.

For no RF reflection, self-actuating RF power (P_{self}) of the switch [12] is given by

$$P_{self} = c_2\frac{V_p^2}{Z_o} \tag{19}$$

where c_2 is constant whose value change from 1 to 0.25 depending upon the series /parallel configurations.

From equations (18) and (19), the power handling of the switch due to self-actuation is

$$P_{self} = c_2\frac{8kg^3}{27\varepsilon_o AZ_o} \tag{20}$$

After scaling, from equation (4) and Table 2, scaled self-actuating power ($P_{self,s}$) decreases by a factor of α^3/β.

$$P_{self,s} = \alpha^2 P_{self} \tag{21}$$

However, using broadside configuration or floating metal [7] or second electrode [8], the problem of self-actuation is controlled. All the switch parameters with scaling factor are listed in Table 3.

Table 3 The effect of the scaling laws on the switch characteristics ($\beta<\alpha<1$)

SN	Parameter	Scaling factor
1	Pull-in voltage	$\sqrt{\frac{\alpha^3}{\beta}}$
2	Spring constant	1
3	Stiction force	β
4	Restoring force	α
5	Mechanical frequency	1/β
6	Switching time	β
7	Energy consumption	α^2
8	Power handling (self-actuation)	α^3/β
9	Area	β

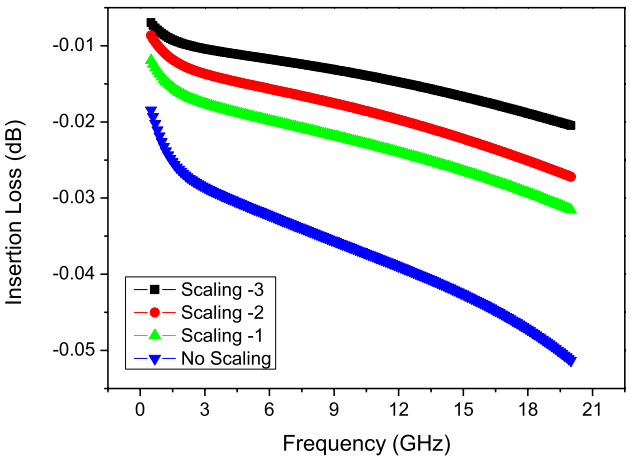

Fig. 7 Change in insertion loss of the switch with scaling

2.8 Electromagnetic response

The electromagnetic response of the proposed ohmic switch is also simulated on high-frequency structural simulator (HFSS) to analyze scaling effects. Both insertion loss and Isolation are improved with scaling as shown in Fig. 7 and Fig. 8.

3 Conclusion

The generalized scaling laws for RF MEMS/NEMS switches are presented. The width of the switch structure is kept constant in the scaling. The length and thickness of the structure are scaled by the same factor (β). The gap between electrode and structure is scaled by a larger factor ($\alpha>\beta$). By going

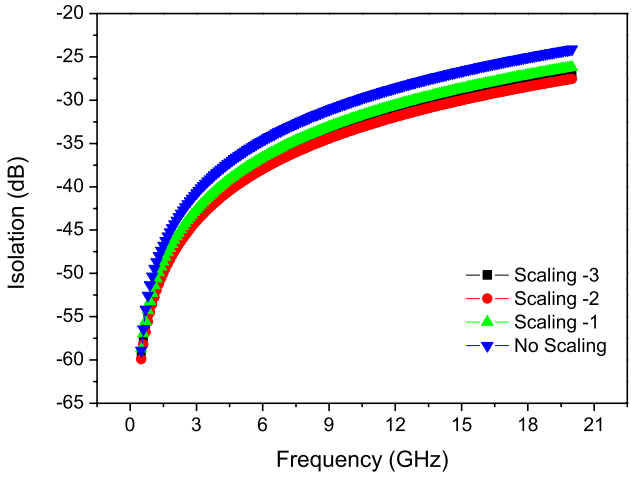

Fig. 8 Change in isolation of the switch with scaling

from MEMS to NEMS, the important mechanical parameters like switching speed, mechanical frequency, and actuation voltage are improved with scaling. The electromagnetic response of the switch like insertion loss and isolation is also improving with scaling.

Compliance with ethical standards

Conflict of interest Authors declare no conflict of interest.

References

1. De Groot, W.A., Webster, J.R., Felnhofer, D., Gusev, E.P.: Review of device and reliability physics of dielectrics in electrostatically driven MEMS devices. IEEE Trans. Device Mater. Reliab. **9**(2), 190–202 (2009). https://doi.org/10.1109/TDMR.2009.2020565
2. Zaghloul, U., Piazza, G.: Highly scalable NEMS relays with stress-tuned switching voltage using piezoelectric buckling actuators. IEEE Trans. Electron Devices **61**(10), 3520–3528 (2014). https://doi.org/10.1109/TED.2014.2331914
3. Wautelet, M.: Scaling laws in the macro, micro and nanoworlds. Eur. J. Phys. **22**(6), 601–611 (2001). https://doi.org/10.1088/0143-0807/22/6/305
4. Trimmer, W.S.N.: Microrobots and micromechanical systems. Sensors and Actuators **19**(3), 267–287 (1989). https://doi.org/10.1016/0250-6874(89)87079-9
5. Bansal, D., Bajpai, A., Kumar, P., Kaur, M., Kumar, A.: Effect of Stress on Pull-in Voltage of RF MEMS SPDT Switch. IEEE Trans. Electron Devices **67**(5), 2147–2152 (2020). https://doi.org/10.1109/ted.2020.2982667
6. Bansal, D., Bajpai, A., Mehta, K., Kumar, P., Kumar, A.: Improved Design of Ohmic RF MEMS Switch for Reduced Fabrication Steps. IEEE Trans. Electron Devices **66**(10), 4361–4366 (2019). https://doi.org/10.1109/TED.2019.2932846
7. Bansal, D., Kumar, A., Sharma, A., Kumar, P., Rangra, K.J.: Design of novel compact anti-stiction and low insertion loss RF MEMS switch. Microsyst. Technol. **20**(2), 337–340 (2013). https://doi.org/10.1007/s00542-013-1812-1
8. Rangra, K., et al.: Symmetric toggle switch—a new type of rf MEMS switch for telecommunication applications: Design and fabrication. Sensors Actuators A Phys. **123–124**, 505–514 (2005). https://doi.org/10.1016/j.sna.2005.03.035
9. Jindal, S.K., Magam, S.P., Shaklya, M.: Analytical modeling and simulation of MEMS piezoresistive pressure sensors with a square silicon carbide diaphragm as the primary sensing element under different loading conditions. J. Comput. Electron. **17**(4), 1780–1789 (2018). https://doi.org/10.1007/s10825-018-1223-8
10. Varma, M.A., Jindal, S.K.: Novel design for performance enhancement of a touch-mode capacitive pressure sensor: theoretical modeling and numerical simulation. J. Comput. Electron. **17**(3), 1324–1333 (2018). https://doi.org/10.1007/s10825-018-1174-0
11. Pu, S.H., Holmes, A.S., Yeatman, E.M., Papavassiliou, C., Lucyszyn, S.: Stable zipping RF MEMS varactors. J. Micromechanics Microengineering **20**(3), 035030 (2010). https://doi.org/10.1088/0960-1317/20/3/035030
12. Rebeiz, G.M.: RF MEMS: Theory, Design, and Technology. John Wiley & Sons Inc, Hoboken, NJ, USA (2003)
13. He, X., et al.: Design and consideration of wafer level micropackaging for distributed RF MEMS phase shifters. Microsyst. Technol. **14**(4–5), 575–579 (2007). https://doi.org/10.1007/s00542-007-0438-6
14. S. Gong, H. Shen, and N. S. Barker (2011) "A 60-GHz 2-bit switched-line phase shifter using SP4T RF-MEMS switches." IEEE Trans Microw Theory Tech. 59(4); 894–900. doi: https://doi.org/10.1109/TMTT.2011.2112374.
15. Bansal, D., Bajpai, A., Kumar, P., Kumar, A., Kaur, M., Rangra, K.: Design and fabrication of a reduced stiction radio frequency MEMS switch. J. Micro/Nanolithography, MEMS, MOEMS **14**(3), 035002 (2015). https://doi.org/10.1117/1.JMM.14.3.035002
16. Van Spengen, W.M., Puers, R., De Wolf, I.: On the physics of stiction and its impact on the reliability of microstructures. J. Adhes. Sci. Technol. **17**(4), 563–582 (2003). https://doi.org/10.1163/15685610360554410
17. a Koszewski, F. Souchon, C. Dieppedale, D. Bloch, and T. Ouisse (2013) "Physical model of dielectric charging in MEMS." J. Micromechanics Microengineering. 23(4); 045019. doi: https://doi.org/10.1088/0960-1317/23/4/045019.
18. Tas, N., Sonnenberg, T., Jansen, H., Legtenberg, R., Elwenspoek, M.: Stiction in surface micromachining. J. Micromechanics Microengineering **6**(4), 385–397 (1996). https://doi.org/10.1088/0960-1317/6/4/005
19. S. Melle et al (2007) "Investigation of Stiction Effect in Electrostatic Actuated RF MEMS Devices." in 2007 Topical Meeting on Silicon Monolithic Integrated Circuits in RF Systems. 21(2); 173–176, doi: https://doi.org/10.1109/SMIC.2007.322787.